Environmental Science & Technology

pubs.acs.org/est

Article

# Assessing the Reactive Surface Area of Soils and the Association of Soil Organic Carbon with Natural Oxide Nanoparticles Using Ferrihydrite as Proxy

Juan C. Mendez,* Tjisse Hiemstra, and Gerwin F. Koopmans

Cite This: *Environ. Sci. Technol.* 2020, 54, 11990−12000

Read Online

ACCESS | Metrics & More | Article Recommendations | Supporting Information

**ABSTRACT:** Assessment of the surface reactivity of natural metal-(hydr)oxide nanoparticles is necessary for predicting ion adsorption phenomena in soils using surface complexation modeling. Here, we describe how the equilibrium concentrations of $PO_4$, obtained with 0.5 M $NaHCO_3$ extractions at different solution-to-soil ratios, can be interpreted with a state-of-the-art ion adsorption model for ferrihydrite to assess the reactive surface area (RSA) of agricultural top soils. Simultaneously, the method reveals the fraction of reversibly adsorbed soil $PO_4$ (R-$PO_4$). The applied ion-probing methodology shows that ferrihydrite is a better proxy than goethite for consistently assessing RSA and R-$PO_4$. The R-$PO_4$ pool agrees well with ammonium oxalate (AO)-extractable phosphorus, but only if measured as orthophosphate. The RSA varied between ∼2 and 20 $m^2$/g soil. The corresponding specific surface area (SSA) of the natural metal-(hydr)oxide fraction is ∼350−1400 $m^2$/g, illustrating that this property is highly variable and cannot be represented by a single value based on the AO-extractable oxide content. The soil organic carbon (SOC) content of our top soils increases linearly not only with the increase in RSA but remarkably also with the increase in mean particle size (1.5−5 nm). To explain these observations, we present a structural model for organo-mineral associations based on the coordination of SOC particles to metal-(hydr)oxide cores.

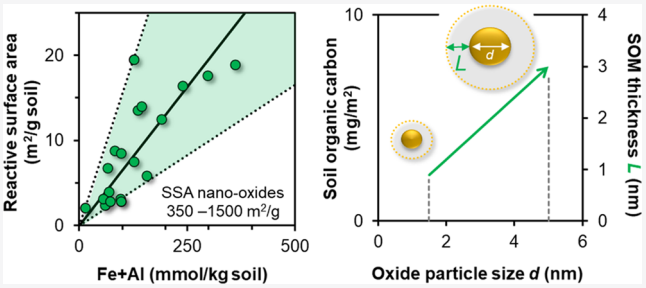


## 1. INTRODUCTION

The chemical behavior of many nutrients and pollutants in the environment is largely controlled by sorption phenomena occurring at the surfaces of metal-(hydr)oxides.[1,2] These surfaces are also crucial for the formation of organo-mineral complexes, contributing to ion adsorption competition[3,4] and to the long-term stabilization of organic carbon in soils and sediments.[5,6] Particularly, nanocrystalline Fe- and Al-(hydr)-oxides may dominate the reactive metal-(hydr)oxide fraction in, for instance, podzols and agricultural top soils.[1,2,7,8]

Surface complexation models (SCMs) are powerful tools for describing ion adsorption to metal-(hydr)oxides. Presently, the charge distribution (CD) model,[9] combined with a multisite ion complexation (MUSIC)[10,11] model, is one of the most advanced SCMs.[12−14] This approach was originally developed using the surface structure of well-crystallized metal-(hydr)-oxides.[9,10,15−17] Recently, it has been extended for modeling ion adsorption to metal-(hydr)oxide nanoparticles, particularly ferrihydrite (Fh),[11,18,19] incorporating recent insights from the mineral and surface structure of this nanomaterial.[18,20−22] The CD-MUSIC framework can also be used for describing the solid-solution partitioning of oxyanions in soils.[7,23−25] However, for a realistic modeling of ion adsorption in soils, information about the reactive surface area (RSA) of the natural metal-(hydr)oxide fraction is an indispensable prerequisite, and therefore, this constitutes the main topic of the present contribution.

An accurate and consistent assessment of the RSA in soil samples is challenging. The use of traditional gas adsorption methods (i.e., Brunauer−Emmett−Teller (BET)) is not suitable because the drying process during sample preparation leads to irreversible aggregation of the metal-(hydr)oxide nanoparticles, resulting in underestimation of the RSA.[26−28] Alternatively, polar compounds (e.g., ethylene glycol mono-ethyl ether) have been used as probe molecules,[29] but this approach typically provides an estimation of the surface area of clays.[30] Humic acids have also been used as probe molecules to determine the relative surface area abundance of goethite and kaolinite in sediments,[31] but this approach has been developed for systems composed of only two mineral phases. For SCM applications to soils, the RSA of the metal-(hydr)oxide fraction is often estimated based on selective extractions of Fe and Al.[23,25,32] In this approach, the nanocrystalline fraction of

Received: April 7, 2020
Revised: September 4, 2020
Accepted: September 9, 2020
Published: September 9, 2020

metal-(hydr)oxides is assessed using a traditional acid ammonium oxalate (AO) extraction[33,34] and next converted to the RSA ($m^2$/g soil) using, for the extracted metal-(hydr)oxides, a standard value for the specific surface area (SSA) and a fixed value for the molar mass ($M_{nano}$). However, this may lead to inconsistent results because both properties are particle size-dependent[35,36] and can greatly vary among soil samples.[37−39]

Hiemstra et al.[7] have developed a probe-ion method for assessing the effective RSA of soils in which soil samples are equilibrated with 0.5 M $NaHCO_3$ (pH 8.5) at different solution-to-soil ratios (SSRs), followed by analysis of the equilibrium $PO_4$ concentration. These data are then interpreted with the CD model to retrieve the RSA, using a chosen metal-(hydr)oxide as a reference to represent the natural metal-(hydr)oxide fraction of soils. At the time of development, well-crystallized goethite was chosen as a proxy because the $PO_4$−$CO_3$ interaction had only been studied extensively for this material.[40] However, the application of this proxy[7,41] revealed for the metal-(hydr)oxide fraction of the studied soils SSA values that are typical for nanosized particles with diameters of ∼2−8 nm, which is in conflict with the use of well-crystallized goethite as a proxy. Recently, the interaction of $PO_4$−$CO_3$ has been measured and modeled for Fh nanoparticles,[42] and we have shown that both oxyanions have rather different competitive adsorption in Fh and goethite systems.[42] This implies that using Fh as a proxy will inevitably affect the RSA of the soil estimated by modeling probe-ion data, and therefore, this will be studied here.

Besides the effective RSA, the above ion-probing methodology also simultaneously reveals the pool of reversibly bound $PO_4$ (R-$PO_4$) that is associated with the metal-(hydr)oxides. This calculated R-$PO_4$ pool can be compared with the pool of orthophosphate extracted with, e.g., ammonium oxalate (AO-$PO_4$). We consider the agreement between R-$PO_4$ and AO-$PO_4$ as a keystone in making the ion-probing methodology a valid and valuable instrument for consistently assessing the RSA of soils. In the earlier approach,[7] it was overlooked that in the data collection total soluble phosphorus ($P_{tot}$) rather than orthophosphate was measured in the AO extracts, while the samples may contain a variable amount of organic P.[43−45] Therefore, in this study, new AO-$PO_4$ data have been collected for the same soils as those used by Hiemstra et al.[7]

The aforementioned ion adsorption framework for Fh includes a systematic implementation of the size dependency of the fundamental properties of this nano-oxide material, including molar mass ($M_{nano}$) and mass density ($\rho_{nano}$), which are both crucial for a consistent interpretation of the ion adsorption data.[46,47] However, in our application of SCM to soils, a complicating factor is that not only Fe but also Al contributes to the composition of the natural metal-(hydr)-oxides. This will affect, among other things, the $M_{nano}$ and particularly the $\rho_{nano}$ of the natural metal-(hydr)oxide fraction. The latter is essential for translating the SSA of the nano-oxide fraction into a corresponding mean particle diameter, which in turn may affect the SCM calculations.[47] In this study, our goal is to develop a systematic and consistent approach for modeling ion adsorption data in soils when this process is governed by Fe- and Al-(hydr)oxide nanoparticles.

Another objective of our study is to gain insights into the close relationship between the calculated RSA and the content of soil organic carbon (SOC) in our top soils. For this purpose, we develop a novel view on how SOC and metal-(hydr)oxide nanoparticles are structurally associated. This is important as these organo-mineral associations are considered as a key factor in determining the long-term stability of SOC.[5,26,48] We show that the variation in the SOC content of our top soils can be largely understood by analyzing the effective RSA of the soil and the SSA of the metal-(hydr)oxide fraction.

## 2. METHODOLOGY

**2.1. Soil Samples.** We used the data set of Hiemstra et al.[7,49] of 19 soil samples, which were selected from a larger collection of representative Dutch agricultural top soils.[50] The selected samples (Table S1) cover a wide range of pH values (∼4.0−7.0), SOC (∼1−15%), clay content (∼3−30%), 0.01 M $CaCl_2$-soluble $PO_4$ (∼1−30 $\mu$M), and Fe- and Al-(hydr)oxides extractable with AO ($[Fe + Al]_{AO}$, 14−361 mmol/kg) and with dithionite−citrate−bicarbonate (DCB) ($[Fe + Al]_{DCB}$, 22−879 mmol/kg).[7]

The above data set[7,49] has been complemented in this study with newly collected data for the orthophosphate concentration in the AO soil extracts (AO-$PO_4$), which was measured colorimetrically[51] with a segmented flow analyzer (SFA) after dilution with demineralized water (×100) to eliminate the interference of oxalate in the AO-$PO_4$ measurements.[43,45] The total soluble phosphorus was also measured in the AO extracts (AO-$P_{tot}$), showing an excellent agreement with previously reported data for the same soil series[7,49] (Figure S1).

**2.2. Phosphate Desorption Data.** The $PO_4$ desorption data are from Hiemstra et al.,[7] which were obtained by equilibrating soil samples (∼10−15 days) with freshly prepared 0.5 M $NaHCO_3$ solutions (pH 8.5) at six SSRs ranging between 5 and 300 L/kg. The equilibrium $PO_4$ concentrations were measured colorimetrically,[51] using an SFA instrument. To remove the dissolved organic matter released during the $NaHCO_3$ extractions, powdered activated carbon (AC) was added (0.40 g/g soil) to the soil suspensions. The detailed experimental procedure is given in Hiemstra et al.[7]

**2.3. Surface Complexation Modeling.** The competitive $PO_4$−$CO_3$ interaction in the 0.5 M $NaHCO_3$ soil extracts was interpreted with a modeling framework built from the combination of the CD model[9] and a novel structural multisite surface complexation (MUSIC) model for Fh.[11] The compact part of the electrical double layer (EDL) was described with the extended Stern layer approach for curved surfaces.[52,53] The solution and surface speciation reactions for Fh are presented in Tables S2 and S3, respectively. The latter includes the complexation of protons, electrolyte ions, $PO_4$, and $CO_3$.[11,42] The pH, $NaHCO_3$ concentration, SSR, and gas-to-solution volume ratio (L/L) were used as input data for the modeling. The effective RSA and R-$PO_4$ were the only adjustable parameters, which were fitted simultaneously by iterative CD model calculations (Section 3.1). Model calculations were done with the software Ecosat[54] (version 4.9) in combination with the FIT[55] program for parameter optimization.

## 3. RESULTS AND DISCUSSION

**3.1. Background.** For a soil, a pool of reversibly bound orthophosphate (R-$PO_4$, mol/kg) can be defined for which the value is fixed at the time of sampling and imposed by the field conditions. Depending on the SSR (L/kg), the R-$PO_4$ pool is redistributed over the solid and solution phases in 0.5 M $NaHCO_3$ extracts according to the mass balance


https://dx.doi.org/10.1021/acs.est.0c02163
Environ. Sci. Technol. 2020, 54, 11990−12000

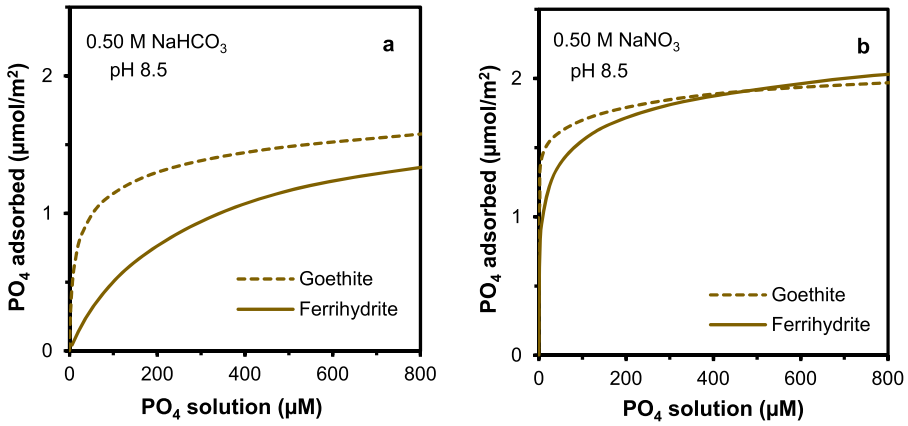


**Figure 1.** $PO_4$ adsorption isotherms of ferrihydrite (full lines) and goethite (dashed lines) in systems with 0.5 M $NaHCO_3$ (a) and 0.5 $NaNO_3$ (b) at pH 8.5, calculated with the CD model, using parameter sets from Hiemstra and Zhao[11] and Mendez and Hiemstra[42] for ferrihydrite and Rahnemaie et al.[40] for goethite.

$$\text{R-PO}_4 = A\Gamma + \text{SSR}\, c \quad (1)$$

where $A$ is the effective RSA of the soil ($m^2$/kg soil), $\Gamma$ is the $PO_4$ surface density of the metal-(hydr)oxide fraction present in the soil (mol/$m^2$), and $c$ is the $PO_4$ concentration in solution (mol/L).

If equilibrium is attained, this mass balance can be used to iteratively derive the surface area $A$ and R-$PO_4$ by measuring the equilibrium concentrations $c_i$ at various $SSR_i$. The measurement of $c$ as a function of SSR results in a $PO_4$ desorption curve, as shown in Figure S2. Key in the methodology to derive $A$ and R-$PO_4$ is the translation of the measured concentrations $c_i$ into the $PO_4$ surface density $\Gamma_i$. Actually, the relationship $\Gamma_i - c_i$ is the competitive adsorption isotherm of $PO_4$ in the $NaHCO_3$ solution, whose interpretation will depend on the type of metal-(hydr)oxide used as reference in the CD model calculations.[42] For a chosen reference oxide, a minimum set of two ($i = 2$) combinations of $c_i$ and $SSR_i$ allows the calculation of the surface area $A$ according to

$$A = \frac{\Delta(\text{SSR}_i \times c_i)}{\Delta\Gamma_i} \quad (2)$$

with $\Delta$ indicating the change in the values of the respective parameters with indices $i$ = 1 and 2.

The calculation of the $PO_4$ surface density is sensitive to uncertainty in the experimental $c$ value in the 0.5 M $NaHCO_3$ extracts. Therefore, six SSRs are used in the present study. These data reveal a part of the desorption isotherm that can be interpreted with the CD model to derive the values of $A$ and R-$PO_4$ by iterative optimization.

**3.2. $PO_4$ Adsorption in Model Systems: Ferrihydrite vs Goethite.** The competitive adsorption isotherm applied in eqs 1 and 2 to relate $\Gamma_i$ and $c_i$ will depend on the type of metal-(hydr)oxide. This implies that the calculation of both $A$ and R-$PO_4$ will be influenced by the choice of either Fh or goethite as reference oxide in the data interpretation of the probe-ion method. Recently, it has been shown that $CO_3$ competes stronger with $PO_4$ for the adsorption to Fh than in the case of goethite.[42] As shown in Figure 1a for a system with 0.5 M $NaHCO_3$ (pH 8.5), the $CO_3$–$PO_4$ interaction is different for goethite and Fh systems, and this difference is $PO_4$-loading-dependent.

In the absence of $CO_3$ as a competitor, the adsorption of $PO_4$ on Fh and goethite is rather similar at pH 8.5, as shown in Figure 1b. However, at lower pH values (e.g., pH 5), Fh adsorbs more $PO_4$ than goethite and this is related to the higher protonation of the adsorbed $PO_4$ species on Fh.[11,56] In 0.5 M $NaHCO_3$ systems (Figure 1a), the adsorption of $PO_4$ to both Fe-(hydr)oxides is lower than in systems with 0.5 M $NaNO_3$ (Figure 1b). This is due to the competition of $CO_3$ and $PO_4$ for the same binding sites at the mineral surfaces. In the presence of $CO_3$, the decrease of the $PO_4$ adsorption is most distinct for Fh (Figure 1a), particularly at low $PO_4$ concentrations, illustrating that $CO_3$ suppresses $PO_4$ adsorption more efficiently on Fh[42] than on goethite.[40,42] Differences in the surface speciation of $CO_3$ might explain the different $CO_3$–$PO_4$ interactions for both oxides. Inner-sphere bidentate complexes dominate the $CO_3$ speciation in both oxides; however, the formation of a ternary complex by the interaction of a $Na^+$ ion with an adsorbed bidentate $CO_3$ complex ($(\equiv FeO)_2CO\cdots Na^+$) is more favored by Fh than by goethite[42] (Figure S3).

In 0.5 M $NaHCO_3$, Fh preserves less well the high-affinity character of $PO_4$ adsorption, which is visible in the form of a lower slope of the isotherm, particularly at low $PO_4$ concentrations. It implies that Fh has a lower capacity to buffer the $PO_4$ concentration in the $NaHCO_3$ solutions. This property will have implications for the probe-ion method in assessing the RSA of soils. Hence, a fundamental question arises: which Fe-(hydr)oxide most accurately represents the ion adsorption behavior of the natural metal-(hydr)oxide fraction of top soils? In other words, which Fe-(hydr)oxide, i.e., Fh or goethite, is a better proxy for the natural oxide fraction in our soils? This is answered in the following section.

**3.3. Reversibly Adsorbed Phosphate: Experimental and Model Results.** For testing which reference Fe-(hydr)oxide material, either Fh or goethite, is a better proxy for describing with SCM the reactivity of the natural metal-(hydr)oxide in top soils, one may collect experimental information regarding the size of the reversibly $PO_4$ pool in soils and compare the results with the calculated R-$PO_4$ pools.

Soil extractions with AO are often used for assessing the fraction of metal-(hydr)oxides present in soils as nanoparticles, because it has been shown that Fh is completely dissolved with that procedure, in contrast to well-crystallized metal-(hydr)-oxides.[1,34,57] The AO extraction method is also used to assess


https://dx.doi.org/10.1021/acs.est.0c02163
Environ. Sci. Technol. 2020, 54, 11990−12000

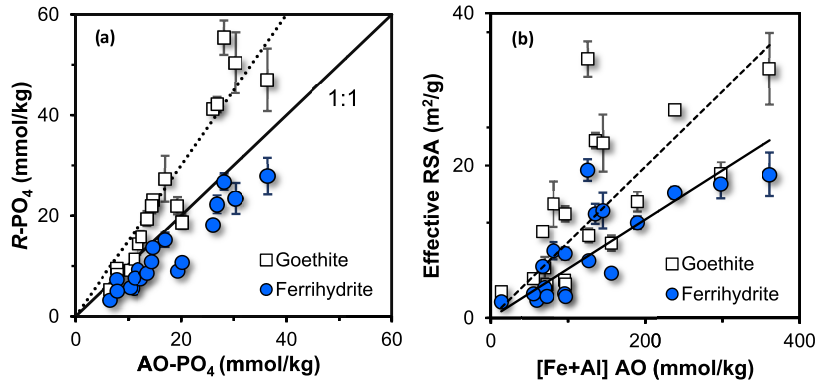


**Figure 2.** (a) Relationship between the amount of acid ammonium oxalate-extractable $PO_4$ (AO-$PO_4$) and the amount reversibly bound $PO_4$ in soils (R-$PO_4$) that has been calculated with the CD model using either goethite (squares) or ferrihydrite (circles) as reference oxide. In the latter case, the data are close to the 1:1 line. (b) Relationship between the ammonium oxalate-extractable Fe and Al contents and the effective reactive surface area (RSA) of the soil samples obtained by modeling the data collected with the probe-ion method, using either goethite (squares) or ferrihydrite (circles) as reference oxide. The slope of the lines in (b) approximates the mean specific surface area (SSA) of the natural metal-(hydr)oxides in soils, which is very high (SSA of ~100 $m^2$/mmol) if goethite is used as reference material. With the use of ferrihydrite as a reference oxide material, a more realistic value for the mean SSA is obtained (SSA of ~65 $m^2$/mmol).

the degree of P saturation of soils[58−60] by measuring with inductively coupled plasma atomic emission spectroscopy (ICP-OES) simultaneously the amount of P released in the AO extracts. Laboratory experiments using a P sink technique have shown that all $P_{tot}$ extractable from soils with AO is potentially desorbable.[61] This $P_{tot}$ pool was also largely available for uptake by grass in a long-term P-mining experiment.[62] However, part of the measured $P_{tot}$ in the AO extracts may not be present as orthophosphate,[43,63] whereas the probe-ion method is based on the measurement of the equilibrium $PO_4$ concentration in the $NaHCO_3$ extracts. Therefore, the molybdenum-blue method[51] has been applied in this study to measure the orthophosphate pool in the AO extracts.[44,45]

For our soils, the difference between the amounts of $P_{tot}$ (AO-$P_{tot}$) and orthophosphate (AO-$PO_4$) as extracted with AO is illustrated in Figure S4a. On average, AO-$PO_4$ contributed to 74 ± 9% to AO-$P_{tot}$. The remainder is probably due to the presence of organic P species ($P_{org}$).[44] Indeed, a positive relationship ($R^2$ = 0.65) is found between $P_{org}$ (i.e., AO-$P_{tot}$ minus AO-$PO_4$) and the SOC content of the soils (Figure S4b).

The presence of $P_{org}$ in the AO extracts implies that the validation of the probe-ion method cannot be based on the comparison of the calculated R-$PO_4$ and the amount of AO-$P_{tot}$, as it was done previously.[7] In other SCM studies, the use of AO-$P_{tot}$ rather than AO-$PO_4$ as a measure for R-$PO_4$ has led to an overestimation of the $PO_4$ concentration in soil leachates[64] and soil-solution extracts.[25] Therefore, the authors proposed the use of isotopically exchangeable $PO_4$ (*E*-value) as a proxy for R-$PO_4$ in SCM. However, the results of this methodology are inherently associated with the kinetics of P exchange and are influenced by the chosen evaluation time.[65]

In Figure 2a, the modeled R-$PO_4$ pools are compared with the experimental measurements of AO-$PO_4$. When goethite is used as reference oxide material in the interpretation of the results of the probe-ion method, the calculated amounts of R-$PO_4$ are on average ~1.5 times larger than the measured amounts of AO-$PO_4$. These model overestimations of the reversibly bound $PO_4$ pool clearly indicate that the $PO_4$ adsorption behavior of the metal-(hydr)oxide fraction of soils in 0.5 M $NaHCO_3$ cannot be well represented by goethite. However, when Fh is used as a reference oxide material, a better agreement is found between modeled and measured amounts of reversibly adsorbed $PO_4$, identifying Fh as a better proxy for the natural metal-(hydr)oxide fraction of our top soils. This suggests that the overall $PO_4$ binding to the natural metal-(hydr)oxide fraction is more similar to the $PO_4$ binding behavior on Fh than to that on goethite. Nevertheless, for some soil samples, the Fh model underestimates the experimental AO-$PO_4$ values, which may be due to the presence of a small fraction of nondesorbable AO-$PO_4$ (e.g., present in an occluded form) or to the presence of more crystalline materials, e.g., nanosized goethite, that contribute to the overall $PO_4$ adsorption.

Additionally, a basic assumption in our approach is that soil organic matter (SOM) does not interfere with the interpretation of the $CO_3$−$PO_4$ competition. Therefore, an excess of activated carbon (AC) is added to remove SOM.[7] Organic P species such as inositol hexa-phosphate (IHP) form coprecipitates with Al, Fe, and Ca,[66] but may also strongly interact with the surfaces of metal-(hydr)oxides in soils, particularly at low pH.[63,67] If the latter fraction is not removed effectively by the AC added to the alkaline $NaHCO_3$ soil extracts, these IHP species can compete with orthophosphate for the same reactive sites, thereby affecting the value of R-$PO_4$.

### 3.4. Reactive Surface Area of Fe and Al-(Hydr)oxides.

Figure 2b shows the effective RSA of our top soils as a function of the amount of AO-extractable Fe and Al ($[Fe + Al]_{AO}$). The RSA, calculated with the CD model using Fh as a proxy for the natural metal-(hydr)oxide fraction, varies by a factor of ~10 across the soil sample series, i.e., ~2−20 $m^2$/g. These RSA values, combined with the $PO_4$ surface density that is simultaneously found by CD modeling, explain the agreement between the experimental AO-$PO_4$ and the modeled R-$PO_4$ values (Figure 2a). This cannot be said when goethite is used as a proxy because in that case more R-$PO_4$ is predicted by modeling than measured in the AO extracts (Figure 2a). In other words, the RSA values found using Fh as a proxy are bona fide.

As expected, the effective RSA and the content of $[Fe + Al]_{AO}$ are positively correlated (Figure 2b). When using Fh as proxy, the slope of the (full) line that approximates the mean value of the specific surface area (SSA) of the soil metal-


https://dx.doi.org/10.1021/acs.est.0c02163
Environ. Sci. Technol. 2020, 54, 11990−12000

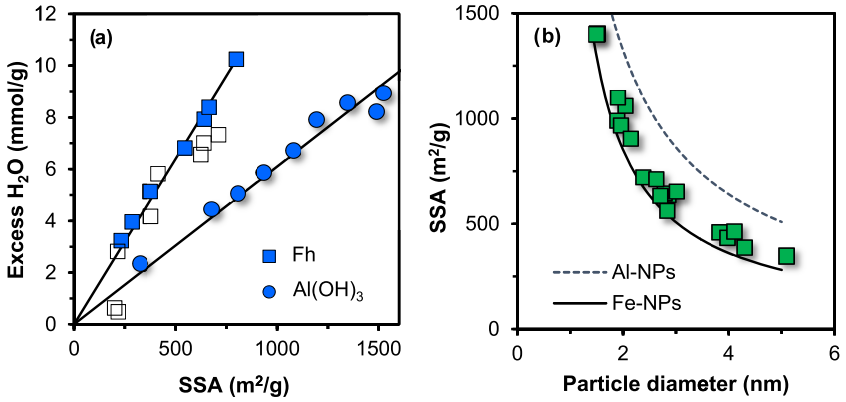


**Figure 3.** (a) Relationship between the specific surface area (SSA) and the excess amount of chemisorbed water of Fh (squares) and $Al(OH)_3$ (circles) nanoparticles, derived by a whole particle construction approach.[82] Open symbols are experimental data for Fh taken from Michel et al.[20] (b) Theoretical relationship between the mean particle diameter and the SSA of Fh (full line) and $Al(OH)_3$ (dotted line) nanoparticles, calculated using the set of mathematical relationships given by Hiemstra[46] and described in Section S6 of the SI. Symbols are for the natural metal-(hydr)oxide fraction of the top soil samples studied here (see the text).

(hydr)oxide fraction is ~65 ± 12 $m^2$/mmol $[Fe + Al]_{AO}$ or ~730 ± 130 $m^2$/g oxide using a mean molar mass of 89 g/mol Fe + Al. In the erroneous case of using goethite, the mean value would be SSA = 1120 ± 250 $m^2$/g oxide. Using $[Fe + Al]_{DCB}$ in the scaling instead of $[Fe + Al]_{AO}$ (Figure S5), these SSA values will decrease because $[Fe + Al]_{AO}$ in our soil samples represents on average ~60 ± 15% of the total metal-(hydr)oxide content (Table S1). The difference $[Fe + Al]_{DCB}$ minus $[Fe + Al]_{AO}$ can be attributed to the presence of well-crystallized metal-(hydr)oxides. However, the SSA of this fraction is likely much lower. Crystalline Fe-(hydr)oxides prepared in the laboratory usually have SSAs that are up to a factor of ~10 smaller than the SSA of Fh.[1,36] Hence, well-crystallized oxides in our top-soil samples may contribute more in terms of mass than in terms of surface reactivity. Indeed, exploratory calculations (Figure S6) suggest that the $[Fe + Al]_{AO}$ fraction represents ~90 ± 10% of the total metal-(hydr)oxide reactivity of our soils on a surface area basis.

The RSA values derived from the probe-ion method represent an "effective" reactive surface area, resulting from probing all surfaces in soil that bind $PO_4$ and for which the adsorption interactions are described using a well-characterized proxy, e.g., Fh in our case. The metal-(hydr)oxide fraction is thought to be the most important reactive material for the binding of $PO_4$ in soils due to its much higher affinity for oxyanions and larger SSA in comparison with other reactive soil surfaces.[24,43,68] For instance, calcium carbonate minerals (e.g., calcite) can also bind $PO_4$,[69] but due to their low binding affinity and SSA, the contribution of these minerals to the effective RSA would be relevant only in strongly calcareous soils with a low metal-(hydr)oxide content. The oxidic edges of clays can also contribute to the calculated RSA, particularly in fine-textured soils.[70] The possible clay contribution to the RSA in our soils can be inferred from the regression analysis of the relationship between RSA and $[Fe + Al]_{AO}$ (Figure 2b), provided that the clay and metal-(hydr)oxide contents are not significantly correlated. A positive and significant intercept of the linear regression line in Figure 2b would then suggest a contribution of clay minerals to the RSA. However, such a contribution cannot be resolved statistically from our data, i.e., the intercept is not significantly different from zero ($p < 0.001$). Therefore, the RSA estimated for our top soils is likely dominated by metal-(hydr)oxides, particularly by the nanocrystalline fraction of Fe- and Al-(hydr)oxides.

The physicochemical properties of naturally formed metal-(hydr)oxide nanoparticles may differ from those of their synthetic counterparts.[1,71] In nature, the nanocrystalline structure and particle size distribution of Fh are affected when it precipitates in the presence of organic matter[72−75] or inorganic ions (e.g., $Al^{3+}$, $Si^{4+}$).[76−78] This has raised concerns about the use of SCMs that are parameterized for synthetic oxides for describing ion adsorption to the metal-(hydr)oxide fraction of soils.[71] However, despite molecular-scale differences found for the binding preferences of $PO_4$ to Al/Fe coprecipitates, the macroscopic adsorption of $PO_4$ was indistinguishable from that of pure Fh at Al/(Fe + Al) molar ratios <0.50,[79] meaning that the adsorption isotherms were similar. Likewise, our results show that the overall macroscopic adsorption behavior of $PO_4$ to metal-(hydr)oxides in soils can be well described using Fh as reference oxide material. From a practical perspective, this study is relevant as it supports the use of Fh as a single proxy for describing the interaction of oxyanions with the reactive fraction of metal-(hydr)oxides in top soils with SCM. Implications of using only Fh as a proxy in the assessment of the effective RSA are discussed in Section 3.5.

Despite the uncertainties associated with the calculation of RSA and R-$PO_4$ with our probe-ion approach, these parameters can be well used in SCM to get for soils more mechanistic insights into the chemical processes affecting the soil-solution partitioning of $PO_4$ in, for instance, equilibrium extractions that are routinely used for assessing the P-status of soils.[80,81]

**3.5. Size-Dependent Properties of Natural Metal-(Hydr)oxides.** Translation of the SSA ($m^2$/mol) to an equivalent mean particle size $d$ (m) of natural metal-(hydr)oxide nanoparticles requires a consistent set of values for the molar mass $M_{nano}$ (g/mol) and mass density $\rho_{nano}$ (g/$m^3$). These values can be assessed using a set of mathematical relationships, as given by Hiemstra.[46] Since $M_{nano}$ and $\rho_{nano}$ are both particle size-dependent, they cannot be calculated directly, but their values are derived iteratively as explained in Section S6 of the Supporting Information (SI).

The $M_{nano}$ and $\rho_{nano}$ of Fe- and Al-(hydr)oxide nanoparticles depend on their chemical composition. For Fh, the chemical


https://dx.doi.org/10.1021/acs.est.0c02163
Environ. Sci. Technol. 2020, 54, 11990−12000

**Table 1. Summary of the Size-Dependent Characteristics of the Nano-oxide Phases Used as Endmembers to Derive the Properties of the Reactive Metal-(Hydr)oxide Nanoparticles for the Set of Top-Soil Samples Used in This Study**

| | | $M_{nano}$ (g/mol)[a] | | $\rho_{nano}$ (g/cm$^3$)[a] | | |
|---|---|---|---|---|---|---|
| | diameter, $d$ (nm) | Fh | $Al(OH)_3$ | Fh | $Al(OH)_3$ | SSA[b] (m$^2$/g oxide) |
| average | 2.83 | 96.6 | 88.9 | 3.78 | 2.30 | 760 |
| min | 1.50 | 87.0 | 82.7 | 3.10 | 2.21 | 350 |
| max | 5.13 | 115.4 | 98.5 | 4.28 | 2.36 | 1400 |

[a]The reactive fraction of metal-(hydr)oxide nanoparticles is assumed to be composed of only Fe- and Al-(hydr)oxides, whose content is estimated from the amount of AO-extractable Fe and Al. The values of $\rho_{nano}$ and $M_{nano}$ are calculated with eqs S1 and S2, respectively, using a single particle diameter for the contributing Fe and Al-(hydr)oxide nanoparticle phases (see Section S6 in the SI). [b]The overall SSA was calculated iteratively and rounded to the nearest 10 (eqs S5 and S6) to account for the size dependency of $\rho_{nano}$ and $M_{nano}$. The SSA of the soil metal-(hydr)oxide fraction is mass-weighted based on the content of Fe- and Al-(hydr)oxides extracted with AO.

composition can be given as $FeO_{1.4}(OH)_{0.2}{\cdot}nH_2O$, where $FeO_{1.4}(OH)_{0.2}$ is the composition of the bulk mineral and $nH_2O$ is the amount of chemisorbed water completing the coordination sphere of the Fe atoms present at the surface.[18,36] Similarly, the composition of nanosized Al-(hydr)oxide particles may be written as $Al(OH)_3{\cdot}nH_2O$. The fraction of metal ions forming surface groups increases when the particle size decreases, leading to an increase in $nH_2O$. Consequently, $M_{nano}$ increases when the particle size decreases, whereas $\rho_{nano}$ simultaneously decreases because the surface groups ($-OH_2$ and $-OH$) contribute more to the particle volume than to the mass.[36]

In Figure 3a, the excess amount of chemisorbed water ($nH_2O$) is presented for Fh and $Al(OH)_3$ nanoparticles as a function of the SSA. For Fh, the data are from Hiemstra.[82] For comparison, experimental Fh data of Michel et al.[20] are also given. The data for $Al(OH)_3$ have been derived in the present study following a whole particle construction approach, as described previously.[18,82] Briefly, near-spherical nanoparticles varying in size are constructed with the Crystalmaker software and the amount of coordinative water of these particles is calculated after completion of the coordination sphere of the metal ions at the surface by adding additional $-OH$ and $-OH_2$ groups.[82] As follows from Figure 3a, the excess amount of water is less for $Al(OH)_3$ nanoparticles than for Fh. The reason is that for $Al(OH)_3$, part of the surface ligands is already present as $-OH$, while this is mainly $-O$ in the case of Fh. The slope of the linear relationships of Figure 3a represents the surface loading of excess chemisorbed water, with $N_{H_2O}$ being 12.6 $\mu$mol/m$^2$ for Fh and $N_{H_2O}$ being 6.3 $\mu$mol/m$^2$ for $Al(OH)_3$.

In Figure 3b, the theoretical relationship between SSA and the equivalent spherical particle diameter $d$, calculated with $SSA = 6/(\rho_{nano}d)$, is given for Fh and $Al(OH)_3$ nanoparticles. For spherical particles with the same diameter, the SSA of $Al(OH)_3$ is higher than that of Fh. The reason is that $Al(OH)_3$ has a much lower $\rho_{nano}$ since the oxygen ions of the lattice are neutralized by light (Al) and very light (H) elements, in contrast to Fh where most neutralizing cations are heavy (Fe).

Figure 3b also shows the equivalent particle diameter ($d$) of the natural metal-(hydr)oxides in the various soils of this study. The calculated $d$ varies between ~1.5 and 5 nm. The smallest particles will contain typically ~50 metal ions and the largest ones ~2000. The calculated $d$ values are between those of Fh and $Al(OH)_3$ because the natural metal-(hydr)oxides contain ~5−50 mol % Al as found in the AO extracts (Table S1). This Al can be partly present in the Fe-(hydr)oxides by Al-substitution.[1] When Fh is synthesized in the presence of increasing amounts of Al, a substitution of up to ~20−30 mol % Al has been reported before the precipitation of secondary Al-(hydr)oxide phases occurred.[83,84]

The $d$ values of the natural metal-(hydr)oxide fraction (Figure 3b) have been calculated by scaling the effective RSA to the amount of $[Fe + Al]_{AO}$. In the approach, the overall SSA of the metal-(hydr)oxide fraction is calculated assuming that the $M_{nano}$ and $\rho_{nano}$ are weighted values of two constituting nano-oxide phases, i.e., Fh and nano-$Al(OH)_3$, that are treated as endmembers in the calculations. The overall $M_{nano}$ and $\rho_{nano}$ of the natural metal-(hydr)oxides are, respectively, the mole-weighted $M_{nano}$ and the volume-weighted $\rho_{nano}$ of the two endmember nano-oxide phases, for which the corresponding $M_{nano}$ and $\rho_{nano}$ values are found with the set of equations given by Hiemstra.[46] Details of the calculation procedure are given in Section S6 of the SI.

Table 1 summarizes the variation in $M_{nano}$ and $\rho_{nano}$ of the constituting nano-(hydr)oxide phases that contribute to the size-dependent properties of the natural metal-(hydr)oxide fraction of our top soils. The SSAs of the reactive metal-(hydr)oxides obtained for our soils (Tables 1 and S1) largely vary, as it ranges between ~350 and 1400 m$^2$/g. Hence, the use of a "standard" SSA value for AO-extractable Fe- and Al-(hydr)oxides, as often done in SCM studies (e.g., 600 m$^2$/g),[25,32,64] may lead to a large deviation in the supposed availability of reactive sites in the soils. This, in turn, will affect the outcome of the ion adsorption modeling.

The $M_{nano}$ values of the nano-oxide endmembers (Table 1) are larger than the molar masses of the bulk minerals, $FeO_{1.4}(OH)_{0.2}$ (81.65 g/mol) and $Al(OH)_3$ (78 g/mol). Using these bulk mineral molar masses will lead to smaller values for $d$ and, correspondingly, to larger values for SSA. Following our consistent approach, the estimated $d$ in our top soils ranges between ~1.5 and 5.0 nm, which is in agreement with previous studies stating that nanosized particles dominate the reactive metal-(hydr)oxide in top soils.[7,38,85] Direct measurements for the size of natural metal-(hydr)oxide nanoparticles in soils are scarce in the literature. Using asymmetric flow field-flow fractionation, a size range of ~2−10 nm was found for Fe-(hydr)oxide nanoparticles from a podzol soil dispersed with pyrophosphate, with maximum concentrations found at a particle size of ~5 nm.[37] These results provided direct evidence for the presence of reactive nanosized particles in the metal-(hydr)oxide fraction of the soil studied.

The effective RSA values used in the above calculations were derived using only Fh as a proxy in the CD model. As mentioned, the macroscopic $PO_4$ adsorption behavior of the reactive metal-(hydr)oxides in our top soils is similar to that of Fh. However, if differences exist in $PO_4$ affinity between Fe-


https://dx.doi.org/10.1021/acs.est.0c02163
Environ. Sci. Technol. 2020, 54, 11990−12000

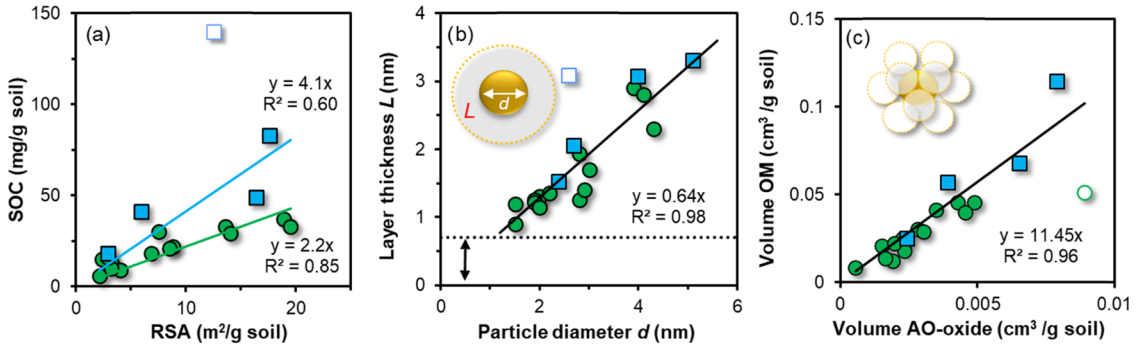


**Figure 4.** (a) Relationship between bulk soil organic carbon (SOC) and effective reactive surface area (RSA) for our mineral top soils with a clay content <20% (circles) and ≥20% (squares). The slope of the lines represents the mean adsorption density of soil organic carbon (SOC). Sample 11 (open symbol) was excluded from the regression analysis due to the exceptionally high SOC content of this peaty soil. (b) Relationship between the layer thickness $L$ of soil organic matter (SOM) and the mean particle diameter ($d$) of the reactive metal-(hydr)oxide fraction, according to a core−shell model (see the inset), showing that larger oxide particles are associated with more organic matter. (c) Relationship between the volumes of SOM and the volumes of the Fe + Al nano-oxide fraction, extractable with AO, both expressed in $cm^3/g$ soil. The open symbol refers to a soil with an exceptionally high Fe + Al oxide content (soil 3) and has been excluded from the calculation of the mean volume ratio $R_v$, which is for our data set $R_v$ = ∼10. If this $R_v$ is interpreted as a coordination number (CN), the arrangement of SOM particles around a metal-(hydr)oxide core varies between cubic (CN = 8) and cub-octahedral (CN = 12). The latter arrangement is shown in the inset.

and Al-(hydr)oxides, this will lead to a systematic bias in the RSA calculations. A larger $PO_4$ adsorption capacity, expressed in mol $PO_4$ per mol Al or Fe, has been reported for nanocrystalline Al-(hydr)oxide compared to that for Fh.[79,86] This may suggest a difference in binding affinity. However, it cannot be excluded that the materials differ in particle size and SSA, rather than in affinity. As the SSA of $Al(OH)_3$ nanomaterials is currently unknown, no parameterized SCM exists to date that can be deployed. This underlines the relevance of the present approach that uses only Fh as proxy for the overall reactive metal-(hydr)oxides in soils. A future challenge will be the development of an SCM approach that distinguishes between nanocrystalline Fe- and Al-(hydr)oxides. This may be particularly relevant for describing the competitive adsorption of $AsO_4$−$PO_4$ as these oxyanions may have different competitive behavior in mixed systems containing both Fe and Al-(hydr)oxides.[43,86]

**3.6. Organo-Mineral Interactions: Structural Arrangement.** In the literature, the relationship between SOC and metal-(hydr)oxide content has been well recognized for various soil types.[26,87,88] With our ion-probe methodology, the relationship between SOC and the calculated values of RSA can now be evaluated, which will help gain more insights into the interaction between natural metal-(hydr)oxide nanoparticles and humic substances. This interaction is important because it contributes to the long-term stabilization of SOC[26,48,89,90] and to the high apparent stability of reactive metal-(hydr)oxide nanoparticles in the environment.[36,91] Moreover, this interaction is important for better understanding the fate of oxyanions in the environment as SOC competes with oxyanions for the binding sites at the surfaces of metal-(hydr)oxides.[23,25,49]

In our set of agricultural top soils, the total SOC content increases as the effective RSA increases. A distinct linear relationship between SOC and RSA is observed when the samples are categorized according to the soil texture (Figure 4a). The slopes of the lines in Figure 4a give the maximum amount of organic carbon that is associated with minerals (MOC). For the soils with a low clay content (<20%), the maximum MOC value is ∼2.2 mg C/$m^2$ oxide. For our soils with a high clay content (≥20%), the maximum MOC value is 2-fold higher (∼4.1 mg C/$m^2$ oxide). Traditionally, this difference has been attributed to an additional contribution of SOC that interacts with the surfaces of clay, for instance via $Ca^{2+}$ bridging.[92,93] This $Ca^{2+}$ bridging plays an important role on the interaction between SOM molecules, clay, and metal-(hydr)oxide particles,[94,95] which may contribute to (micro)-aggregate formation that promotes the stabilization of SOC.[8,88,93]

To sketch the contours of the interaction of SOC with metal-(hydr)oxide nanoparticles, a conceptual mineral core−surface layer model can be considered in which all SOM is accommodated in a layer around the metal-(hydr)oxide nanoparticles, as shown in the inset in Figure 4b. The implemented approach for calculating the layer thickness $L$ of SOM is given in Section S10 of the SI. This approach leads for our top soils to fitted $L$ values between ∼1 and 3 nm (Figure 4b). These $L$ values are thicker than the thickness of the compact part of the electrical double layer (EDL), i.e., ∼0.7 nm[52] (dotted line, Figure 4b). As shown in Figure 4b, only the smallest metal-(hydr)oxide nanoparticles with a low layer thickness $L$ can accommodate a significant fraction of the total SOM closely to the surface, in the compact part of the EDL.

Remarkably, the calculated layer thickness $L$ increases linearly ($R^2$ = 0.98, $p$ < 0.001) with an increase in the mean diameter of the metal-(hydr)oxide nanoparticles, as given in Figure 4b. If this is due to a physical and/or chemical protection of SOM against microbial decomposition,[5,26,48] the relationship suggests a more efficient SOM protection when particles are relatively large. This picture might be understood from a more robust structural organization of the organo-mineral particles forming larger microaggregates.

The SOM−mineral interaction can also be interpreted with another structural picture in which the organo-mineral association is seen as a collection of more discrete particles of metal-(hydr)oxide and SOM. A significant relationship is found ($R^2$ = 0.96, $p$ < 0.001) between the volume of both types of particles, yielding a volume ratio ($R_v$) of ∼10. This $R_v$ is high in comparison to the value of ∼1 estimated from the maximum adsorption of SOM to synthetic Fe-(hydr)oxides.[96,97] If the mean $R_v$ value from Figure 4c is interpreted as a particle coordination number (CN), the structural arrangement of the


https://dx.doi.org/10.1021/acs.est.0c02163
Environ. Sci. Technol. 2020, 54, 11990−12000

organo-mineral associations varies between a cubic (CN = 8) and a cub-octahedral (CN = 12) configuration. According to Pauling's first rule, the CN can be related to the ratio of particle radii being 0.73 (CN = 8) and 1.0 (CN = 12). These radii ratios suggest that the particles in the organo-mineral entities are similar in size. An increase in the size of the mineral nanoparticles is accompanied by a corresponding increase in the mean size of the SOM particles, and this results in a constant $R_v$ (Figure 4c). Once formed, the organo-mineral entities may be organized at a higher structural level, forming aggregates that are more robust in encountering microbial degradation.

## ■ ASSOCIATED CONTENT

### Supporting Information

The Supporting Information is available free of charge at https://pubs.acs.org/doi/10.1021/acs.est.0c02163.

Properties of the selected soil samples (Section S1), consistency of total P measurements in the ammonium oxalate extracts (Section S2), thermodynamic databases used in the modeling (Section S3), results of the probe-ion method (0.5 M $NaHCO_3$ extractions) (Section S4), surface speciation of $CO_3$ in competitive systems with $PO_4$ (Section S5), calculation of size-dependent properties of metal-(hydr)oxide nanoparticles (Section S6), orthophosphate vs organic phosphorus in the ammonium oxalate soil extracts (Section S7), relationship of RSA- vs DCB-extractable Fe- and Al-(hydr)oxides (Section S8), relative contribution of the nanocrystalline and crystalline metal-(hydr)oxides (Section S9), and calculation of SOM layer thickness (Section S10) (PDF)

## ■ AUTHOR INFORMATION


### Corresponding Author

**Juan C. Mendez** − *Soil Chemistry and Chemical Soil Quality Group, Wageningen University and Research, 6700 AA Wageningen, The Netherlands;* orcid.org/0000-0002-1658-400X; Phone: +31 317 48 2342; Email: juan.mendezfernandez@wur.nl

### Authors

**Tjisse Hiemstra** − *Soil Chemistry and Chemical Soil Quality Group, Wageningen University and Research, 6700 AA Wageningen, The Netherlands*

**Gerwin F. Koopmans** − *Soil Chemistry and Chemical Soil Quality Group, Wageningen University and Research, 6700 AA Wageningen, The Netherlands*

Complete contact information is available at: https://pubs.acs.org/10.1021/acs.est.0c02163


### Author Contributions

The manuscript was written through the contributions of all authors. All authors have given approval to the final version of the manuscript.

### Notes

The authors declare no competing financial interest.

## ■ ACKNOWLEDGMENTS

We gratefully acknowledge the financial support of the University of Costa Rica.

## ■ REFERENCES


(1) Cornell, R. M.; Schwertmann, U. *The Iron Oxides: Structure, Properties, Reactions, Ocurrence and Uses*, 2nd ed.; Wiley-VCH: Germany, 2003.

(2) Guo, H.; Barnard, A. S. Naturally Occurring Iron Oxide Nanoparticles: Morphology, Surface Chemistry and Environmental Stability. *J. Mater. Chem. A* **2013**, *1*, 27−42.

(3) Xue, Q.; Ran, Y.; Tan, Y.; Peacock, C. L.; Du, H. Arsenite and Arsenate Binding to Ferrihydrite Organo-Mineral Coprecipitate: Implications for Arsenic Mobility and Fate in Natural Environments. *Chemosphere* **2019**, *224*, 103−110.

(4) Weng, L.; van Riemsdijk, W. H.; Hiemstra, T. Humic Nanoparticles at the Oxide−Water Interface: Interactions with Phosphate Ion Adsorption. *Environ. Sci. Technol.* **2008**, *42*, 8747−8752.

(5) Kleber, M.; Eusterhues, K.; Keiluweit, M.; Mikutta, C.; Mikutta, R.; Nico, P. S. Mineral-Organic Associations: Formation, Properties, and Relevance in Soil Environments. *Adv. Agron.* **2015**, *130*, 1−140.

(6) Lalonde, K.; Mucci, A.; Ouellet, A.; Gélinas, Y. Preservation of Organic Matter in Sediments Promoted by Iron. *Nature* **2012**, *483*, 198−200.

(7) Hiemstra, T.; Antelo, J.; Rahnemaie, R.; van Riemsdijk, W. H. Nanoparticles in Natural Systems I: The Effective Reactive Surface Area of the Natural Oxide Fraction in Field Samples. *Geochim. Cosmochim. Acta* **2010**, *74*, 41−58.

(8) Pronk, G. J.; Heister, K.; Kögel-Knabner, I. Iron Oxides as Major Available Interface Component in Loamy Arable Topsoils. *Soil Sci. Soc. Am. J.* **2011**, *75*, 2158−2168.

(9) Hiemstra, T.; Van Riemsdijk, W. H. A Surface Structural Approach to Ion Adsorption: The Charge Distribution (CD) Model. *J. Colloid Interface Sci.* **1996**, *179*, 488−508.

(10) Hiemstra, T.; Venema, P.; Van Riemsdijk, W. H. Intrinsic Proton Affinity of Reactive Surface Groups of Metal (Hydr)Oxides: The Bond Valence Principle. *J. Colloid Interface Sci.* **1996**, *184*, 680−692.

(11) Hiemstra, T.; Zhao, W. Reactivity of Ferrihydrite and Ferritin in Relation to Surface Structure, Size, and Nanoparticle Formation Studied for Phosphate and Arsenate. *Environ. Sci. Nano* **2016**, *3*, 1265−1279.

(12) Komárek, M.; Antelo, J.; Králová, M.; Veselská, V.; Číhalová, S.; Chrastný, V.; Ettler, V.; Filip, J.; Yu, Q.; Fein, J. B.; Koretsky, C. M. Revisiting Models of Cd, Cu, Pb and Zn Adsorption onto Fe(III) Oxides. *Chem. Geol.* **2018**, *493*, 189−198.

(13) Groenenberg, J. E.; Lofts, S. The Use of Assemblage Models to Describe Trace Element Partitioning, Speciation, and Fate: A Review. *Environ. Toxicol. Chem.* **2014**, *33*, 2181−2196.

(14) Koopal, L.; Tan, W.; Avena, M. Equilibrium Mono- and Multicomponent Adsorption Models: From Homogeneous Ideal to Heterogeneous Non-Ideal Binding. *Adv. Colloid Interface Sci.* **2020**, No. 102138.

(15) Hiemstra, T.; Yong, H.; Van Riemsdijk, W. H. Interfacial Charging Phenomena of Aluminum (Hydr)Oxides. *Langmuir* **1999**, *15*, 5942−5955.

(16) Machesky, M. L.; Wesolowski, D. J.; Palmer, D. A.; Ridley, M. K. On the Temperature Dependence of Intrinsic Surface Protonation Equilibrium Constants: An Extension of the Revised MUSIC Model. *J. Colloid Interface Sci.* **2001**, *239*, 314−327.

(17) Machesky, M. L.; Předota, M.; Wesolowski, D. J.; Vlcek, L.; Cummings, P. T.; Rosenqvist, J.; Ridley, M. K.; Kubicki, J. D.; Bandura, A. V.; Kumar, N.; Sofo, J. O. Surface Protonation at the Rutile (110) Interface: Explicit Incorporation of Solvation Structure within the Refined MUSIC Model Framework. *Langmuir* **2008**, *24*, 12331−12339.

(18) Hiemstra, T. Surface and Mineral Structure of Ferrihydrite. *Geochim. Cosmochim. Acta* **2013**, *105*, 316−325.

(19) Hiemstra, T. Surface Structure Controlling Nanoparticle Behavior: Magnetism of Ferrihydrite, Magnetite, and Maghemite. *Environ. Sci. Nano* **2018**, *5*, 752−764.

(20) Michel, F. M.; Barron, V.; Torrent, J.; Morales, M. P.; Serna, C. J.; Boily, J.-F.; Liu, Q.; Ambrosini, A.; Cismasu, A. C.; Brown, G. E. Ordered Ferrimagnetic Form of Ferrihydrite Reveals Links among Structure, Composition, and Magnetism. *Proc. Natl. Acad. Sci. U.S.A.* **2010**, *107*, 2787−2792.
(21) Michel, F. M.; Ehm, L.; Antao, S. M.; Lee, P. L.; Chupas, P. J.; Liu, G.; Strongin, D. R.; Schoonen, M. A. A.; Phillips, B. L.; Parise, J. B. The Structure of Ferrihydrite, a Nanocrystalline Material. *Science* **2007**, *316*, 1726−1729.
(22) Harrington, R.; Hausner, D. B.; Xu, W.; Bhandari, N.; Michel, F. M.; Brown, G. E.; Strongin, D. R.; Parise, J. B. Neutron Pair Distribution Function Study of Two-Line Ferrihydrite. *Environ. Sci. Technol.* **2011**, *45*, 9883−9890.
(23) Gustafsson, J. P. Arsenate Adsorption to Soils: Modelling the Competition from Humic Substances. *Geoderma* **2006**, *136*, 320−330.
(24) Weng, L.; Vega, F. A.; van Riemsdijk, W. H. Competitive and Synergistic Effects in PH Dependent Phosphate Adsorption in Soils: LCD Modeling. *Environ. Sci. Technol.* **2011**, *45*, 8420−8428.
(25) Verbeeck, M.; Hiemstra, T.; Thiry, Y.; Smolders, E. Soil Organic Matter Reduces the Sorption of Arsenate and Phosphate: A Soil Profile Study and Geochemical Modelling. *Eur. J. Soil Sci.* **2017**, *68*, 678−688.
(26) Kaiser, K.; Guggenberger, G. The Role of DOM Sorption to Mineral Surfaces in the Preservation of Organic Matter in Soils. *Org. Geochem.* **2000**, *31*, 711−725.
(27) Strehlau, J. H.; Toner, B. M.; Arnold, W. A.; Penn, R. L. Accessible Reactive Surface Area and Abiotic Redox Reactivity of Iron Oxyhydroxides in Acidic Brines. *Geochim. Cosmochim. Acta* **2017**, *197*, 345−355.
(28) Heister, K. The Measurement of the Specific Surface Area of Soils by Gas and Polar Liquid Adsorption Methods—Limitations and Potentials. *Geoderma* **2014**, *216*, 75−87.
(29) Cihacek, L. J.; Bremner, J. M. A Simplified Ethylene Glycol Monoethyl Ether Procedure for Assessment of Soil Surface Area1. *Soil Sci. Soc. Am. J.* **1979**, *43*, 821.
(30) Kennedy, M. J.; Pevear, D. R.; Hill, R. J. Mineral Surface Control of Organic Carbon in Black Shale. *Science* **2002**, *295*, 657−660.
(31) Dong, W.; Wan, J. Additive Surface Complexation Modeling of Uranium(VI) Adsorption onto Quartz-Sand Dominated Sediments. *Environ. Sci. Technol.* **2014**, *48*, 6569−6577.
(32) Bonten, L. T. C.; Groenenberg, J. E.; Weng, L.; van Riemsdijk, W. H. Use of Speciation and Complexation Models to Estimate Heavy Metal Sorption in Soils. *Geoderma* **2008**, *146*, 303−310.
(33) Schwertmann, U. Differenzierung Der Eisenoxide Des Bodens Durch Extraktion Mit Ammoniumoxalat-Lösung. *Z. Pflanzenernaehr., Dueng., Bodenkd.* **1964**, *105*, 194−202.
(34) Borggaard, O. K. Dissolution of Poorly Crystalline Iron Oxides in Soils by EDTA and Oxalate. *Z. Pflanzenernaehr. Bodenkd.* **1992**, *155*, 431−436.
(35) Hochella, M. F.; Lower, S. K.; Maurice, P. A.; Penn, R. L.; Sahai, N.; Sparks, D. L.; Twining, B. S. Nanominerals, Mineral Nanoparticles, and Earth Systems. *Science* **2008**, *319*, 1631−1635.
(36) Hiemstra, T.; Mendez, J. C.; Li, J. Evolution of the Reactive Surface Area of Ferrihydrite: Time, PH, and Temperature Dependency of Growth by Ostwald Ripening. *Environ. Sci. Nano* **2019**, *6*, 820−833.
(37) Regelink, I. C.; Weng, L.; Koopmans, G. F.; van Riemsdijk, W. H. Asymmetric Flow Field-Flow Fractionation as a New Approach to Analyse Iron-(Hydr)Oxide Nanoparticles in Soil Extracts. *Geoderma* **2013**, *202*−*203*, 134−141.
(38) Eusterhues, K.; Rumpel, C.; Kögel-Knabner, I. Organo-Mineral Associations in Sandy Acid Forest Soils: Importance of Specific Surface Area, Iron Oxides and Micropores. *Eur. J. Soil Sci.* **2005**, *56*, 753−763.
(39) Theng, B. K. G.; Yuan, G. Nanoparticles in the Soil Environment. *Elements* **2008**, *4*, 395−399.
(40) Rahnemaie, R.; Hiemstra, T.; van Riemsdijk, W. H. Carbonate Adsorption on Goethite in Competition with Phosphate. *J. Colloid Interface Sci.* **2007**, *315*, 415−425.
(41) Koopmans, G. F. F.; Hiemstra, T.; Vaseur, C.; Chardon, W. J. J.; Voegelin, A.; Groenenberg, J. E. E. Use of Iron Oxide Nanoparticles for Immobilizing Phosphorus In-Situ: Increase in Soil Reactive Surface Area and Effect on Soluble Phosphorus. *Sci. Total Environ.* **2020**, *711*, No. 135220.
(42) Mendez, J. C.; Hiemstra, T. Carbonate Adsorption to Ferrihydrite: Competitive Interaction with Phosphate for Use in Soil Systems. *ACS Earth Space Chem.* **2019**, *3*, 129−141.
(43) Cui, Y.; Weng, L. Arsenate and Phosphate Adsorption in Relation to Oxides Composition in Soils: LCD Modeling. *Environ. Sci. Technol.* **2013**, *47*, 7269−7276.
(44) Wolf, A. M.; Baker, D. E. Colorimetric Method for Phosphorus Measurement in Ammonium Oxalate Soil Extracts. *Commun. Soil Sci. Plant Anal.* **1990**, *21*, 2257−2263.
(45) Hass, A.; Loeppert, R. H.; Messina, M. G.; Rogers, T. D. Determination of Phosphate in Selective Extractions for Soil Iron Oxides by the Molybdenum Blue Method in an Automated Continuance Flow Injection System. *Commun. Soil Sci. Plant Anal.* **2011**, *42*, 1619−1635.
(46) Hiemstra, T. Ferrihydrite Interaction with Silicate and Competing Oxyanions: Geometry and Hydrogen Bonding of Surface Species. *Geochim. Cosmochim. Acta* **2018**, *238*, 453−476.
(47) Mendez, J. C.; Hiemstra, T. Surface Area of Ferrihydrite Consistently Related to Primary Surface Charge, Ion Pair Formation, and Specific Ion Adsorption. *Chem. Geol.* **2020**, *532*, No. 119304.
(48) Wagai, R.; Mayer, L. M. Sorptive Stabilization of Organic Matter in Soils by Hydrous Iron Oxides. *Geochim. Cosmochim. Acta* **2007**, *71*, 25−35.
(49) Hiemstra, T.; Antelo, J.; van Rotterdam, A. M. D.; van Riemsdijk, W. H. Nanoparticles in Natural Systems II: The Natural Oxide Fraction at Interaction with Natural Organic Matter and Phosphate. *Geochim. Cosmochim. Acta* **2010**, *74*, 59−69.
(50) van Erp, P. J.; Houba, Y. J. G.; Van Beusichem, M. L. One Hundredth Molar Calcium Chloride Extraction Procedure. Part I: A Review of Soil Chemical, Analytical, and Plant Nutritional Aspects. *Commun. Soil Sci. Plant Anal.* **1998**, *29*, 1603−1623.
(51) Murphy, J.; Riley, J. P. A Modified Single Solution Method for the Determination of Phosphate in Natural Waters. *Anal. Chim. Acta* **1962**, *27*, 31−36.
(52) Hiemstra, T.; Van Riemsdijk, W. H. On the Relationship between Charge Distribution, Surface Hydration, and the Structure of the Interface of Metal Hydroxides. *J. Colloid Interface Sci.* **2006**, *301*, 1−18.
(53) Hiemstra, T.; Van Riemsdijk, W. H. A Surface Structural Model for Ferrihydrite I: Sites Related to Primary Charge, Molar Mass, and Mass Density. *Geochim. Cosmochim. Acta* **2009**, *73*, 4423−4436.
(54) Keizer, M. G.; van Riemsdijk, W. H. *ECOSAT, Equilibrium Calculation of Speciation and Transport*, Technical Report; Department of Soil Quality, Wageningen Univeristy, 1998.
(55) Kinniburgh, D. G. *FIT*, Technical Report WD/93/23; British Geological Survey: Keyworth, 1993.
(56) Rahnemaie, R.; Hiemstra, T.; Van Riemsdijk, W. H. Geometry, Charge Distribution, and Surface Speciation of Phosphate on Goethite. *Langmuir* **2007**, *23*, 3680−3689.
(57) Schwertmann, U.; Schulze, D. G.; Murad, E. Identification of Ferrihydrite in Soils by Dissolution Kinetics, Differential X-Ray Diffraction, and Mössbauer Spectroscopy1. *Soil Sci. Soc. Am. J.* **1982**, *46*, 869−875.
(58) van der Zee, S. E. A. T. M.; van Riemsdijk, W. H. Model for Long-Term Phosphate Reaction Kinetics in Soil. *J. Environ. Qual.* **1988**, *17*, 35−41.
(59) Koopmans, G. F.; Chardon, W. J.; De Willigen, P.; Van Riemsdijk, W. H. Phosphorus Desorption Dynamics in Soil and the Link to a Dynamic Concept of Bioavailability. *J. Environ. Qual.* **2004**, *33*, 1393−1402.


https://dx.doi.org/10.1021/acs.est.0c02163
*Environ. Sci. Technol.* 2020, 54, 11990−12000

(60) Maguire, R. O.; Foy, R. H.; Bailey, J. S.; Sims, J. T. Estimation of the Phosphorus Sorption Capacity of Acidic Soils in Ireland. *Eur. J. Soil Sci.* **2001**, *52*, 479−487.
(61) Lookman, R.; Freese, D.; Merckx, R.; Vlassak, K.; van Riemsdijk, W. H. Long-Term Kinetics of Phosphate Release from Soil. *Environ. Sci. Technol.* **1995**, *29*, 1569−1575.
(62) Koopmans, G. F.; Chardon, W. J.; Ehlert, P. A. I.; Dolfing, J.; Suurs, R. A. A.; Oenema, O.; van Riemsdijk, W. H. Phosphorus Availability for Plant Uptake in a Phosphorus-Enriched Non-calcareous Sandy Soil. *J. Environ. Qual.* **2004**, *33*, 965−975.
(63) Jørgensen, C.; Turner, B. L.; Reitzel, K. Identification of Inositol Hexakisphosphate Binding Sites in Soils by Selective Extraction and Solution 31P NMR Spectroscopy. *Geoderma* **2015**, *257*−*258*, 22−28.
(64) Warrinnier, R.; Goossens, T.; Amery, F.; Vanden Nest, T.; Verbeeck, M.; Smolders, E. Investigation on the Control of Phosphate Leaching by Sorption and Colloidal Transport: Column Studies and Multi-Surface Complexation Modelling. *Appl. Geochem.* **2019**, *100*, 371−379.
(65) Frossard, E.; Sinaj, S. The Isotope Exchange Kinetic Technique: A Method to Describe the Availability of Inorganic Nutrients. Applications to K, P, S and Zn. *Isot. Environ. Health Stud.* **1997**, *33*, 61−77.
(66) Turner, B. L.; Papházy, M. J.; Haygarth, P. M.; Mckelvie, I. D. Inositol Phosphates in the Environment. *Philos. Trans. R. Soc., B* **2002**, *357*, 449−469.
(67) Prietzel, J.; Klysubun, W.; Werner, F. Speciation of Phosphorus in Temperate Zone Forest Soils as Assessed by Combined Wet-Chemical Fractionation and Xanes Spectroscopy. *J. Plant Nutr. Soil Sci.* **2016**, *179*, 168−185.
(68) Goldberg, S. Competitive Adsorption of Arsenate and Arsenite on Oxides and Clay Minerals. *Soil Sci. Soc. Am. J.* **2002**, *66*, 413.
(69) Sø, H. U.; Postma, D.; Jakobsen, R.; Larsen, F. Sorption of Phosphate onto Calcite; Results from Batch Experiments and Surface Complexation Modeling. *Geochim. Cosmochim. Acta* **2011**, *75*, 2911−2923.
(70) Gérard, F. Clay Minerals, Iron/Aluminum Oxides, and Their Contribution to Phosphate Sorption in Soils — A Myth Revisited. *Geoderma* **2016**, *262*, 213−226.
(71) Perret, D.; Gaillard, J. F.; Dominik, J.; Atteia, O. The Diversity of Natural Hydrous Iron Oxides. *Environ. Sci. Technol.* **2000**, *34*, 3540−3546.
(72) Chen, C.; Dynes, J. J.; Wang, J.; Sparks, D. L. Properties of Fe-Organic Matter Associations via Coprecipitation versus Adsorption. *Environ. Sci. Technol.* **2014**, *48*, 13751−13759.
(73) Chen, K. Y.; Chen, T. Y.; Chan, Y. T.; Cheng, C. Y.; Tzou, Y. M.; Liu, Y. T.; Teah, H. Y. Stabilization of Natural Organic Matter by Short-Range-Order Iron Hydroxides. *Environ. Sci. Technol.* **2016**, *50*, 12612−12620.
(74) Eusterhues, K.; Wagner, F. E.; Häusler, W.; Hanzlik, M.; Knicker, H.; Totsche, K. U.; Kögel-Knabner, I.; Schwertmann, U. Characterization of Ferrihydrite-Soil Organic Matter Coprecipitates by X-Ray Diffraction and Mössbauer Spectroscopy. *Environ. Sci. Technol.* **2008**, *42*, 7891−7897.
(75) Mikutta, R.; Lorenz, D.; Guggenberger, G.; Haumaier, L.; Freund, A. Properties and Reactivity of Fe-Organic Matter Associations Formed by Coprecipitation versus Adsorption: Clues from Arsenate Batch Adsorption. *Geochim. Cosmochim. Acta* **2014**, *144*, 258−276.
(76) Cismasu, A. C.; Levard, C.; Michel, F. M.; Brown, G. E. Properties of Impurity-Bearing Ferrihydrite II: Insights into the Surface Structure and Composition of Pure, Al- and Si-Bearing Ferrihydrite from Zn(II) Sorption Experiments and Zn K-Edge X-Ray Absorption Spectroscopy. *Geochim. Cosmochim. Acta* **2013**, *119*, 46−60.
(77) Lee, S.; Xu, H. One-Step Route Synthesis of Siliceous Six-Line Ferrihydrite: Implication for the Formation of Natural Ferrihydrite. *ACS Earth Space Chem.* **2019**, *3*, 503−509.
(78) Hofmann, A.; Vantelon, D.; Montargès-Pelletier, E.; Villain, F.; Gardoll, O.; Razafitianamaharavo, A.; Ghanbaja, J. Interaction of Fe(III) and Al(III) during Hydroxylation by Forced Hydrolysis: The Nature of Al-Fe Oxyhydroxy Co-Precipitates. *J. Colloid Interface Sci.* **2013**, *407*, 76−88.
(79) Liu, Y. T.; Hesterberg, D. Phosphate Bonding on Noncrystalline Al/Fe-Hydroxide Coprecipitates. *Environ. Sci. Technol.* **2011**, *45*, 6283−6289.
(80) Houba, V. J. G.; Temminghoff, E. J. M.; Gaikhorst, G. A.; van Vark, W. Soil Analysis Procedures Using 0.01 M Calcium Chloride as Extraction Reagent. *Commun. Soil Sci. Plant Anal.* **2000**, *31*, 1299−1396.
(81) Koopmans, G. F.; Chardon, W. J.; Dekker, P. H. M.; Römkens, P. F. A. M.; Schoumans, O. F. Comparing Different Extraction Methods for Estimating Phosphorus Solubility in Various Soil Types. *Soil Sci.* **2006**, *171*, 103−116.
(82) Hiemstra, T. Formation, Stability, and Solubility of Metal Oxide Nanoparticles: Surface Entropy, Enthalpy, and Free Energy of Ferrihydrite. *Geochim. Cosmochim. Acta* **2015**, *158*, 179−198.
(83) Adra, A.; Morin, G.; Ona-Nguema, G.; Menguy, N.; Maillot, F.; Casiot, C.; Bruneel, O.; Lebrun, S.; Juillot, F.; Brest, J. Arsenic Scavenging by Aluminum-Substituted Ferrihydrites in a Circumneutral PH River Impacted by Acid Mine Drainage. *Environ. Sci. Technol.* **2013**, *47*, 12784−12792.
(84) Cismasu, A. C.; Michel, F. M.; Stebbins, J. F.; Levard, C.; Brown, G. E. Properties of Impurity-Bearing Ferrihydrite I. Effects of Al Content and Precipitation Rate on the Structure of 2-Line Ferrihydrite. *Geochim. Cosmochim. Acta* **2012**, *92*, 275−291.
(85) Kiem, R.; Kögel-Knabner, I. Refractory Organic Carbon in Particle-Size Fractions of Arable Soils II: Organic Carbon in Relation to Mineral Surface Area and Iron Oxides in Fractions < 6 Mm. *Org. Geochem.* **2002**, *33*, 1699−1713.
(86) Tiberg, C.; Sjöstedt, C.; Eriksson, A. K.; Klysubun, W.; Gustafsson, J. P. Phosphate Competition with Arsenate on Poorly Crystalline Iron and Aluminum (Hydr)Oxide Mixtures. *Chemosphere* **2020**, *255*, No. 126937.
(87) Kleber, M.; Mikutta, R.; Torn, M. S.; Jahn, R. Poorly Crystalline Mineral Phases Protect Organic Matter in Acid Subsoil Horizons. *Eur. J. Soil Sci.* **2005**, *56*, 717−725.
(88) Wiseman, C. L. S.; Püttmann, W. Interactions between Mineral Phases in the Preservation of Soil Organic Matter. *Geoderma* **2006**, *134*, 109−118.
(89) Eusterhues, K.; Neidhardt, J.; Hädrich, A.; Küsel, K.; Totsche, K. U. Biodegradation of Ferrihydrite-Associated Organic Matter. *Biogeochemistry* **2014**, *119*, 45−50.
(90) Mikutta, R.; Kleber, M.; Torn, M. S.; Jahn, R. Stabilization of Soil Organic Matter: Association with Minerals or Chemical Recalcitrance? *Biogeochemistry* **2006**, *77*, 25−56.
(91) Hu, S.; Lu, Y.; Peng, L.; Wang, P.; Zhu, M.; Dohnalkova, A. C.; Chen, H.; Lin, Z.; Dang, Z.; Shi, Z. Coupled Kinetics of Ferrihydrite Transformation and As(V) Sequestration under the Effect of Humic Acids: A Mechanistic and Quantitative Study. *Environ. Sci. Technol.* **2018**, *52*, 11632−11641.
(92) Lutzow, M. v.; Kogel-Knabner, I.; Ekschmitt, K.; Matzner, E.; Guggenberger, G.; Marschner, B.; Flessa, H. Stabilization of Organic Matter in Temperate Soils: Mechanisms and Their Relevance under Different Soil Conditions - a Review. *Eur. J. Soil Sci.* **2006**, *57*, 426−445.
(93) Wattel-Koekkoek, E. J. W.; Van Genuchten, P. P. L.; Buurman, P.; Van Lagen, B. Amount and Composition of Clay-Associated Soil Organic Matter in a Range of Kaolinitic and Smectitic Soils. *Geoderma* **2001**, *99*, 27−49.
(94) Sowers, T. D.; Adhikari, D.; Wang, J.; Yang, Y.; Sparks, D. L. Spatial Associations and Chemical Composition of Organic Carbon Sequestered in Fe, Ca, and Organic Carbon Ternary Systems. *Environ. Sci. Technol.* **2018**, *52*, 6936−6944.
(95) Mikutta, R.; Mikutta, C.; Kalbitz, K.; Scheel, T.; Kaiser, K.; Jahn, R. Biodegradation of Forest Floor Organic Matter Bound to


https://dx.doi.org/10.1021/acs.est.0c02163
*Environ. Sci. Technol.* 2020, 54, 11990−12000

Minerals via Different Binding Mechanisms. *Geochim. Cosmochim. Acta* **2007**, *71*, 2569−2590.
(96) Kaiser, K.; Guggenberger, G. Sorptive Stabilization of Organic Matter by Microporous Goethite: Sorption into Small Pores vs. Surface Complexation. *Eur. J. Soil Sci.* **2007**, *58*, 45−59.
(97) Weng, L. P.; Van Riemsdijk, W. H.; Hiemstra, T. Adsorption of Humic Acids onto Goethite: Effects of Molar Mass, PH and Ionic Strength. *J. Colloid Interface Sci.* **2007**, *314*, 107−118.



https://dx.doi.org/10.1021/acs.est.0c02163
*Environ. Sci. Technol.* 2020, 54, 11990−12000